JOURNAL OF GUIDANCE, CONTROL, AND DYNAMICS
Vol. 25, No. 5, September–October 2002

In-Space Calibration of a Skewed Gyro Quadruplet

Itzhack Y. Bar-Itzhack* and Richard R. Harman†
NASA Goddard Space Flight Center, Greenbelt, Maryland 20771

A new approach to gyro calibration is presented, where the spacecraft dynamics equation, attitude measurements, and the gyro outputs are used in a pseudolinear Kalman filter that estimates the calibration parameters. Also an algorithm is presented for calibrating a skewed quadruplet rather than the customary triad gyro set aligned along the body coordinate axes. In particular, a new misalignment error model is derived for this case. The new calibration algorithm is applied to the EOS-AQUA satellite gyros. The effectiveness of the new algorithm is demonstrated through simulations.

Introduction

GYRO calibration, as well as calibration of other instruments, includes two stages. During the first stage, the instrument error parameters are estimated, and in the second stage, those errors are continuously removed from the gyro readings. In the classical approach to gyro calibration, the gyro outputs are used to maintain or compute body orientation rather than used as measurements in the context of filtering. In inertial navigation, for example,[1] gyro errors cause erroneous computation of velocity and position, and then when the latter are compared to measured velocity and position, a great portion of the computed velocity and position errors can be determined. The latter errors are then fed into a Kalman filter (KF) that uses the inertial navigation system error model to infer the gyro errors. Similarly, when applying the classical approach to spacecraft (SC) attitude determination, the gyro outputs are used to compute the attitude, and then the attitude measurements[2,3] are used to determine the attitude errors, which again using a KF indicates what the gyro errors are.

Several ways of treating gyro calibration have been presented in the literature.[4–6] In the approach adopted in this work, the gyro outputs are used as angular rate measurements and are compared to estimated angular rates. However, this approach requires the knowledge of the angular rate. In the past,[7] the estimated angular rate was computed in a rather simplistic way, assuming basically that the rate was constant. In the present work, the estimated angular rate is derived using a KF whose input can be any kind of attitude measurement; therefore, the angular rate experienced by the SC can be continuously changing, and yet a good estimate of the rate, necessary for calibration, can be obtained.

The calibration algorithm presented in this work was derived for a set of quadruplet gyros. This required the derivation of a new error model, particularly for the gyro misalignments. The new calibration algorithm was applied to the gyro package of the EOS-AQUA satellite. The latter consists of four gyros, which are given the task of measuring the three components of the SC angular velocity vector resolved in the body Cartesian coordinates.

Received 10 October 2001; revision received 12 March 2002; accepted for publication 14 May 2002.

*National Research Council Resident Research Associate, Flight Dynamics Analysis Branch, Code 572, Guidance Navigation and Control Center; on sabbatical leave, Sophie and William Shamban Professor of Aerospace Engineering, Faculty of Aerospace Engineering, Technion—Israel Institute of Technology, 32000 Haifa, Israel; ibaritz@pop500.gsfc.nasa.gov. Fellow AIAA.

†Aerospace Engineer, Flight Dynamics Analysis Branch, Code 572, Guidance Navigation and Control Center; richard.r.harman.1@gsfc.nasa.gov.

In the next section, the gyro error model is derived. The section that follows presents an algorithm for computing the calibration parameters when the rate is known, and then in the section that follows, we present the same when the rates are unknown. In the following section, we present the compensation procedure that needs to take place to complete the calibration process, and in the subsequent section, we present simulation results. Finally, in the last section, the conclusions are presented.

Gyro Error Model

The gyro errors that are considered in this work are misalignment, scale factor error, and bias (constant drift rate). The gyro error model is basically a linear model, which associates small error sources to the gyro outputs. Because of the linearity of the model we can compute the contribution of each error source independently and then sum up all of the contributions into one linear model.

We start the description of the error model, by deriving the expression for the gyro misalignments.

Misalignment Model

The assumed direction of the sensitive axis of gyro j, which is one of the four gyros, is presented in Fig. 1, where the body coordinate axes are also presented and are denoted by $\boldsymbol{X}$, $\boldsymbol{Y}$, and $\boldsymbol{Z}$. The orientation of this gyro is expressed by a vector of unit length in the direction of the gyro sensitive axis. The direction of this unit vector in the body coordinates is expressed by its three direction cosines, which are identical to its components when the unit vector is resolved in the body coordinates. These components are c_{j1}, c_{j2}, and c_{j3}. Inasmuch as they are direction cosines, or equivalently, components of a unit vector, the sum of their squares adds up to 1, that is,

$$c_{j1}^2 + c_{j2}^2 + c_{j3}^2 = 1 \tag{1}$$

The rate that this gyro reads is the projection of the angular velocity vector on this unit vector. If we express the angular velocity vector in the body coordinates, where its components are ω_x, ω_y, and ω_z, then this projection is given by

$$\mathbf{1}_j \cdot \boldsymbol{\omega}_b = c_{j1}\omega_x + c_{j2}\omega_y + c_{j3}\omega_z \tag{2a}$$

where $\mathbf{1}_j$ is the unit vector along the jth gyro sensitive axis and $\boldsymbol{\omega}_b$ is the angular rate vector. The nominal (errorless) reading of this gyro is then

$$G_{jn} = c_{j1}\omega_x + c_{j2}\omega_y + c_{j3}\omega_z = [c_{j1} \quad c_{j2} \quad c_{j3}]\begin{bmatrix}\omega_x \\ \omega_y \\ \omega_z\end{bmatrix} \tag{2b}$$

where the subscript n denotes the nominal or design value. Combining all four gyros, we obtain

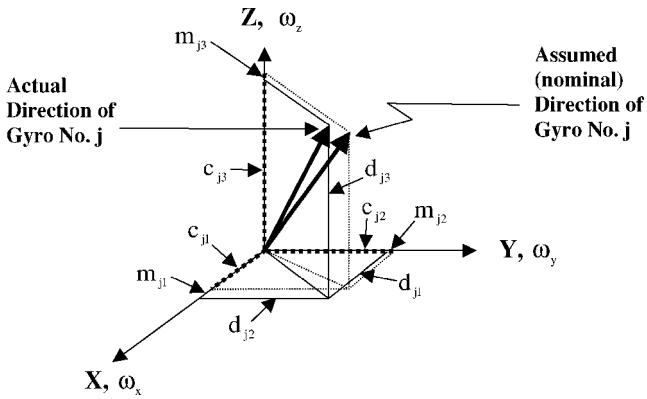

Fig. 1 Geometry of assumed and actual direction of the gyro input axis.

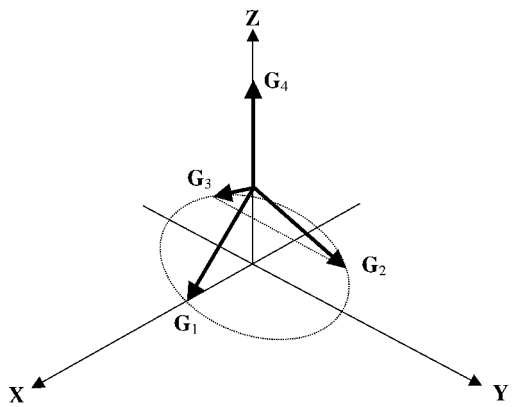

Fig. 2 Gyro configuration in the EOS-AQUA satellite.

$$\begin{bmatrix} G_{1n} \\ G_{2n} \\ G_{3n} \\ G_{4n} \end{bmatrix} = \begin{bmatrix} c_{11} & c_{12} & c_{13} \\ c_{21} & c_{22} & c_{23} \\ c_{31} & c_{32} & c_{33} \\ c_{41} & c_{42} & c_{43} \end{bmatrix} \begin{bmatrix} \omega_x \\ \omega_y \\ \omega_z \end{bmatrix} \tag{3a}$$

Define

$$\boldsymbol{G}_n^T = [G_{1n} \quad G_{2n} \quad G_{3n} \quad G_{4n}] \tag{3b}$$

$$C = \begin{bmatrix} c_{11} & c_{12} & c_{13} \\ c_{21} & c_{22} & c_{23} \\ c_{31} & c_{32} & c_{33} \\ c_{41} & c_{42} & c_{43} \end{bmatrix} \tag{3c}$$

Equation (3a) can be written as

$$\boldsymbol{G}_n = C\boldsymbol{\omega}_b \tag{4}$$

In the EOS-AQUA satellite, the gyro configuration is as shown in Fig. 2, where, as mentioned before, $\boldsymbol{X}$, $\boldsymbol{Y}$, and $\boldsymbol{Z}$ are the axes of the body frame. The C matrix in this case is

$$C = \begin{bmatrix} \sqrt{\frac{2}{3}} & 0 & -\sqrt{\frac{1}{3}} \\ -\sqrt{\frac{1}{6}} & \sqrt{\frac{1}{2}} & -\sqrt{\frac{1}{3}} \\ -\sqrt{\frac{1}{6}} & -\sqrt{\frac{1}{2}} & -\sqrt{\frac{1}{3}} \\ 0 & 0 & 1 \end{bmatrix} \tag{5}$$

Note that the vector described by each row is of unit length as it should be [see Eq. (1)].

Because of misalignment, the sensitive axis of each gyro may actually point at a slightly different direction than the assumed one. This is shown in Fig. 1, where the components of this direction

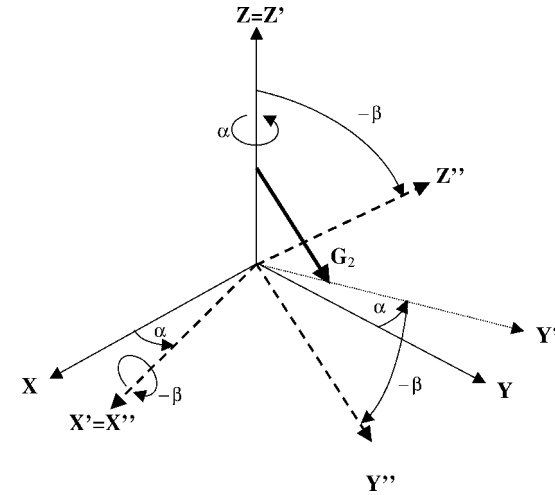

Fig. 3 Transformation from the G_2 body to gyro coordinates.

(which is still a unit vector) are d_{j1}, d_{j2}, and d_{j3}, respectively. When the steps that led to the development of the nominal gyro reading presented in Eq. (2b) are followed, the actual gyro reading is found to be

$$G_{ja} = d_{j1}\omega_x + d_{j2}\omega_y + d_{j3}\omega_z = [d_{j1} \quad d_{j2} \quad d_{j3}] \begin{bmatrix} \omega_x \\ \omega_y \\ \omega_z \end{bmatrix} \tag{6}$$

where the subscript a denotes an actual value. The difference ΔG_j between the reading of the jth gyro and its assumed nominal reading is computable using Eqs. (2b) and (6) as follows:

$$\Delta G_j^m = G_{ja} - G_{jn} = [d_{j1} - c_{j1} \quad d_{j2} - c_{j2} \quad d_{j3} - c_{j3}] \begin{bmatrix} \omega_x \\ \omega_y \\ \omega_z \end{bmatrix} \tag{7}$$

where the superscript m denotes that the error is due to misalignment. We denote by m_{ji} the differences $d_{j1} - c_{j1}$, $d_{j2} - c_{j2}$, and $d_{j3} - c_{j3}$ as follows:

$$m_{j1} = d_{j1} - c_{j1} \tag{8a}$$

$$m_{j2} = d_{j2} - c_{j2} \tag{8b}$$

$$m_{j3} = d_{j3} - c_{j3} \tag{8c}$$

Using Eqs. (8), we can write Eq. (7) as follows:

$$\Delta G_j^m = [\omega_x \quad \omega_y \quad \omega_z] \begin{bmatrix} m_{j1} \\ m_{j2} \\ m_{j3} \end{bmatrix} \tag{9}$$

The m_{ji} differences are shown in Fig. 1. Actually only two of the m_{ji} of each gyro are independent. This results from that the nominal as well as the actual directions of the gyros are given by vectors of unit length. For a reason that will become clear later, let us choose to present the third component of m_j by the first two, that is, we express m_{j3}, the misalignment along the sensitive axis, as a function of m_{j1} and m_{j2}. Because, similarly to Eq. (1), it is also true that

$$d_{j1}^2 + d_{j2}^2 + d_{j3}^2 = 1 \tag{10}$$

then using this relation and Eq. (8c), we can write

$$m_{j3} = \sqrt{1 - d_{j1}^2 - d_{j2}^2} - \sqrt{1 - c_{j1}^2 - c_{j2}^2} \tag{11}$$

For the case described by the fourth gyro (G_4 in Fig. 3), the nominal direction of the gyro sensitive axis is along the Z axis; therefore, $c_{41} = c_{42} = 0$. Then from Eqs. (8a) and (8b),

$$m_{41} = d_{41} \tag{12a}$$

$$m_{42} = d_{42} \tag{12b}$$

and from Eq. (11),

$$m_{43} = \sqrt{1 - d_{41}^2 - d_{42}^2} - 1 \tag{13}$$

In the case where the misalignments are small, d_{41}^2 and d_{42}^2 are small, too. Therefore, we can expand the square root function of Eq. (11) in a Taylor series as follows:

$$\sqrt{1 - d_{41}^2 - d_{42}^2} \approx 1 - \tfrac{1}{2}d_{41}^2 - \tfrac{1}{2}d_{42}^2 \tag{14}$$

(Note that the linear term of the series vanishes.) Substitution of the last equation into Eq. (13) yields

$$m_{43} = -\tfrac{1}{2}d_{41}^2 - \tfrac{1}{2}d_{42}^2 = -\tfrac{1}{2}m_{41}^2 - \tfrac{1}{2}m_{42}^2 \tag{15}$$

When d_{41} and d_{42} are indeed small, such as this case, then m_{43} is negligible with respect to m_{41} and m_{42}. Then using Eqs. (12), we can write

$$\begin{bmatrix} m_{41} \\ m_{42} \\ m_{43} \end{bmatrix} = \begin{bmatrix} 1 & 0 \\ 0 & 1 \\ 0 & 0 \end{bmatrix} \begin{bmatrix} d_{41} \\ d_{42} \end{bmatrix} \tag{16}$$

It is the choice to express the component of m_j, which lies along the gyro sensitive axis (in this case m_{43}) that enables its elimination.

For gyros whose sensitive axes are not aligned along one of the body axes, the computation is more elaborate. Consider, for example, G_2, the second gyro of the EOS-AQUA satellite. To define its misalignment in the body coordinates, let us define a coordinate system in which the nominal gyro sensitive axis is aligned along one of its axes. Such a system ($\boldsymbol{X}''$, $\boldsymbol{Y}''$, $\boldsymbol{Z}''$) is presented in Fig. 3, where the sensitive axis of the G_2 gyro is aligned along the system $\boldsymbol{Y}''$ axis. Following the preceding development for the G_4 gyro, we conclude that

$$m_{21}'' = d_{21}'' \tag{17a}$$

$$m_{23}'' = d_{23}'' \tag{17b}$$

$$m_{22}'' = -\tfrac{1}{2}d_{21}''^2 - \tfrac{1}{2}d_{23}''^2 = -\tfrac{1}{2}m_{21}''^2 - \tfrac{1}{2}m_{23}''^2 \tag{17c}$$

(The double prime sign denotes that the values are expressed in the $\boldsymbol{X}''$, $\boldsymbol{Y}''$, and $\boldsymbol{Z}''$ coordinate system.) Here, too, the misalignment along the sensitive axis m_{22}'' is normally negligible. To compute the misalignment error in the gyro reading, we have to use Eq. (9), where the angular rate vector is transformed to the double-prime coordinate system, and the misalignment parameters are those given in Eqs. (17a) and (17b). As shown in Fig. 3, the transformation from the body to the double-prime coordinates is performed by two rotations. The first rotation is by an angle α about the $\boldsymbol{Z}$ axis, and the second is by an angle $-\beta$ about the $\boldsymbol{X}'$ axis. (Note that with this sign definition the numerical value of β has to be positive for this geometry.) The resulting transformation matrix from the body to the G_2 coordinates is, therefore,

$$R_2^b = \begin{bmatrix} c\alpha & s\alpha & 0 \\ -s\alpha \cdot c\beta & c\alpha \cdot c\beta & -s\beta \\ -s\alpha \cdot s\beta & c\alpha \cdot s\beta & c\beta \end{bmatrix} \tag{18}$$

$$\boldsymbol{\omega}_2 = R_2^b \boldsymbol{\omega}_b \tag{19}$$

when Eq. (9) is followed and Eqs. (17a–17c) are used,

$$\Delta G_2^m = \left[R_2^b \boldsymbol{\omega}_b\right]^T \boldsymbol{d}_{2^*}'' = \boldsymbol{\omega}_b^T R_b^2 \boldsymbol{d}_{2^*}'' \tag{20}$$

where

$$[\boldsymbol{d}_{2^*}'']^T = [d_{21}'' \quad 0 \quad d_{23}''] \tag{21}$$

It is easy to see that

$$R_b^2 \boldsymbol{d}_{2^*}'' = \begin{bmatrix} c\alpha & -s\alpha \cdot s\beta \\ s\alpha & c\alpha \cdot s\beta \\ 0 & c\beta \end{bmatrix} \begin{bmatrix} d_{21}'' \\ d_{23}'' \end{bmatrix} \tag{22}$$

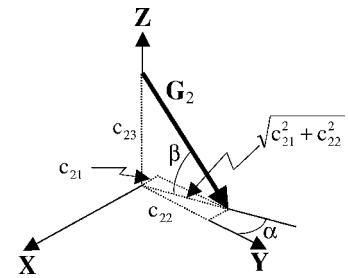

Fig. 4 Definition of the rotation angles α and β.

Define

$$E_2 = \begin{bmatrix} c\alpha & -s\alpha \cdot s\beta \\ s\alpha & c\alpha \cdot s\beta \\ 0 & c\beta \end{bmatrix} \tag{23a}$$

$$\boldsymbol{d}_2 = \begin{bmatrix} d_{21}'' \\ d_{23}'' \end{bmatrix} \tag{23b}$$

then Eq. (20) can be written as

$$\Delta G_2^m = \boldsymbol{\omega}_b^T E_2 \boldsymbol{d}_2 \tag{24}$$

To evaluate E_2, we need to compute the angles α and β. For this we turn to Fig. 4, where these angles are defined by the projection of the G_2 direction on the body axes. From Fig. 4, we conclude that

$$\alpha = \tan^{-1}(|c_{21}/c_{22}|) \tag{25a}$$

$$\beta = \cos^{-1}\left(\sqrt{c_{21}^2 + c_{22}^2}/1\right) = \cos^{-1}\left(\sqrt{c_{21}^2 + c_{22}^2}\right) \tag{25b}$$

Using the EOS-AQUA satellite values [see Eqs. (4) and (5)], we obtain

$$\alpha = \tan^{-1}(|c_{21}/c_{22}|) = \tan^{-1}\left(\sqrt{\tfrac{1}{6}}/\sqrt{\tfrac{1}{2}}\right)$$
$$= \tan^{-1}\left(1/\sqrt{3}\right) = 30 \text{ deg} \tag{25c}$$

$$\beta = \cos^{-1}\left(\sqrt{c_{21}^2 + c_{22}^2}\right) = \cos^{-1}\left(\sqrt{\tfrac{1}{6} + \tfrac{1}{2}}\right)$$
$$= \cos^{-1}\left(\sqrt{\tfrac{2}{3}}\right) = 35.26 \text{ deg} \tag{25d}$$

Because of the symmetry between the positioning of the G_2 and the G_3 gyros, it is easy to see that, when considering G_3, the first rotation is about the body $\boldsymbol{Z}$ axis by the angle $\pi - \alpha$ and then about the $\boldsymbol{X}'$ axis by the angle $-\beta$. Therefore,

$$R_3^b = \begin{bmatrix} -c\alpha & s\alpha & 0 \\ -s\alpha \cdot c\beta & -c\alpha \cdot c\beta & -s\beta \\ -s\alpha \cdot s\beta & -c\alpha \cdot s\beta & c\beta \end{bmatrix} \tag{26}$$

and similarly to Eq. (19), for this transformation we obtain

$$\boldsymbol{\omega}_3 = R_3^b \boldsymbol{\omega}_b \tag{27}$$

and then, following Eq. (20),

$$\Delta G_3^m = \left[R_3^b \boldsymbol{\omega}_b\right]^T \boldsymbol{d}_{3^*}'' = \boldsymbol{\omega}_b^T R_b^3 \boldsymbol{d}_{3^*}'' \tag{28}$$

where

$$[\boldsymbol{d}_{3^*}'']^T = \left[d_{31}'' \quad 0 \quad d_{33}''\right] \tag{29}$$

It is easy to see that

$$R_b^3 \boldsymbol{d}_{3^*}'' = \begin{bmatrix} -c\alpha & -s\alpha \cdot s\beta \\ s\alpha & -c\alpha \cdot s\beta \\ 0 & c\beta \end{bmatrix} \begin{bmatrix} d_{31}'' \\ d_{33}'' \end{bmatrix} \tag{30}$$

Define

$$E_3 = \begin{bmatrix} -c\alpha & -s\alpha \cdot s\beta \\ s\alpha & -c\alpha \cdot s\beta \\ 0 & c\beta \end{bmatrix} \tag{31a}$$

$$\boldsymbol{d}_3 = \begin{bmatrix} d''_{31} \\ d''_{33} \end{bmatrix} \tag{31b}$$

then Eq. (28) can be written as

$$\Delta G_3^m = \boldsymbol{\omega}_b^T E_3 \boldsymbol{d}_3 \tag{32}$$

For the G_1 gyro, we have only one rotation, which brings the body $\boldsymbol{X}$ axis into coincidence with the G_1 gyro sensitive axis (Fig. 2). It is about the $\boldsymbol{Y}$ axis by an angle, which we denote by γ. For this gyro, we have then

$$R_1^b = \begin{bmatrix} c\gamma & 0 & -s\gamma \\ 0 & 1 & 0 \\ s\gamma & 0 & c\gamma \end{bmatrix} \tag{33}$$

and the angular rate in coordinate system 1 is then

$$\boldsymbol{\omega}_1 = R_1^b \boldsymbol{\omega}_b \tag{34}$$

thus,

$$\Delta G_1^m = \left[R_1^b \boldsymbol{\omega}_b\right]^T d''_{1*} = \boldsymbol{\omega}_b^T R_b^1 \boldsymbol{d}'_{1*} \tag{35}$$

where

$$[\boldsymbol{d}'_{1*}]^T = [0 \quad d'_{12} \quad d'_{13}] \tag{36}$$

We denote the misalignment parameters of this gyro by a single prime because it takes only one rotation (to a single-prime system) to align the coordinate axis with the nominal sensitive axis of the G_1 gyro. Note that here the misalignments that are not negligible are d'_{12} and d'_{13}, and it is easy to see that

$$R_b^1 \boldsymbol{d}''_{1*} = \begin{bmatrix} 0 & -s\gamma \\ 1 & 0 \\ 0 & c\gamma \end{bmatrix} \begin{bmatrix} d'_{12} \\ d'_{13} \end{bmatrix} \tag{37}$$

Define

$$E_1 = \begin{bmatrix} 0 & -s\gamma \\ 1 & 0 \\ 0 & c\gamma \end{bmatrix} \tag{38a}$$

$$\boldsymbol{d}_1 = \begin{bmatrix} d''_{12} \\ d''_{13} \end{bmatrix} \tag{38b}$$

then Eq. (35) can be written as

$$\Delta G_1^m = \boldsymbol{\omega}_b^T E_1 \boldsymbol{d}_1 \tag{39}$$

From Fig. 2, it is easy to see that the rotation angle γ is computable as follows:

$$\gamma = \sin^{-1}(|c_{13}|/1) = \sin^{-1}\left(\sqrt{\tfrac{1}{3}}\right) = 35.26 \text{ deg} \tag{40}$$

Similarly to the computations carried out for the misalignment errors for gyros 1, 2, and 3, we can write for gyro 4

$$\Delta G_4^m = \boldsymbol{\omega}_b^T E_4 \boldsymbol{d}_4 \tag{41}$$

where, based on Eq. (16),

$$E_4 = \begin{bmatrix} 1 & 0 \\ 0 & 1 \\ 0 & 0 \end{bmatrix} \tag{42a}$$

$$\boldsymbol{d}_4 = \begin{bmatrix} d_{41} \\ d_{42} \end{bmatrix} \tag{42b}$$

Let

$$[\Delta \boldsymbol{G}^m]^T = \begin{bmatrix} \Delta G_1^m & \Delta G_2^m & \Delta G_3^m & \Delta G_4^m \end{bmatrix} \tag{43a}$$

$$\Omega^m = \begin{bmatrix} \omega_x & \omega_y & \omega_z & 0 & 0 & 0 & 0 & 0 & 0 & 0 & 0 & 0 \\ 0 & 0 & 0 & \omega_x & \omega_y & \omega_z & 0 & 0 & 0 & 0 & 0 & 0 \\ 0 & 0 & 0 & 0 & 0 & 0 & \omega_x & \omega_y & \omega_z & 0 & 0 & 0 \\ 0 & 0 & 0 & 0 & 0 & 0 & 0 & 0 & 0 & \omega_x & \omega_y & \omega_z \end{bmatrix} \tag{43b}$$

$$E = \begin{bmatrix} E_1 & 0 & 0 & 0 \\ 0 & E_2 & 0 & 0 \\ 0 & 0 & E_3 & 0 \\ 0 & 0 & 0 & E_4 \end{bmatrix} \tag{43c}$$

$$\boldsymbol{d}^T = \begin{bmatrix} \boldsymbol{d}_1^T & \boldsymbol{d}_2^T & \boldsymbol{d}_3^T & \boldsymbol{d}_4^T \end{bmatrix} \tag{43d}$$

Then Eqs. (39), (24), (32), and (41) can be unified into the following single equation:

$$\Delta \boldsymbol{G}^m = \Omega^m E \boldsymbol{d} \tag{44}$$

In the Appendix, we apply the general misalignment model presented here to a special case where the gyro sensitive axes are placed along the body axes and show that the obtained results are the well-known results for this case.

Scale Factor Error Model

As mentioned, another error source that causes the difference between the correct value of the rates and their measurements is the scale factor errors. The error model for the scale factor error is simply

$$\Delta \boldsymbol{G}^k = \begin{bmatrix} \omega_{G1} k_1 \\ \omega_{G2} k_2 \\ \omega_{G3} k_3 \\ \omega_{G4} k_4 \end{bmatrix} \tag{45}$$

where the superscript k denotes that this error is caused by gyro scale factor error; ω_{Gi}, $i = 1$–4, is the angular velocity measured by gyro number i; and k_i is the scale factor error of that gyro. The actual components ω_{Gi} are obtained by transforming the angular velocity expressed in body coordinates to the actual misaligned gyro sensitive axes using the matrix D [the jth row of D is shown in Eq. (6)]; however, because D is unknown to us, we use instead the matrix C that transforms the body rate to the nominal gyro axes and is close enough to D. Thus, we use

$$\begin{bmatrix} \omega_{G1} \\ \omega_{G2} \\ \omega_{G3} \\ \omega_{G4} \end{bmatrix} = C \begin{bmatrix} \omega_x \\ \omega_y \\ \omega_z \end{bmatrix} \tag{46}$$

where in the case of EOS-AQUA, C is as given in Eq. (5). Equation (45) can be written as follows:

$$\Delta \boldsymbol{G}^k = \begin{bmatrix} \omega_{G1} & 0 & 0 & 0 \\ 0 & \omega_{G2} & 0 & 0 \\ 0 & 0 & \omega_{G3} & 0 \\ 0 & 0 & 0 & \omega_{G4} \end{bmatrix} \begin{bmatrix} k_1 \\ k_2 \\ k_3 \\ k_4 \end{bmatrix} \tag{47}$$

Define

$$\Omega^k = \begin{bmatrix} \omega_{G1} & 0 & 0 & 0 \\ 0 & \omega_{G2} & 0 & 0 \\ 0 & 0 & \omega_{G3} & 0 \\ 0 & 0 & 0 & \omega_{G4} \end{bmatrix} \tag{48a}$$

$$\boldsymbol{k}^T = [k_1 \quad k_2 \quad k_3 \quad k_4] \tag{48b}$$

then Eq. (47) can be written as

$$\Delta \boldsymbol{G}^k = \Omega^k \boldsymbol{k} \tag{48c}$$

Bias Model

The bias error model is quite simple and is given by

$$b = \begin{bmatrix} b_1 \\ b_2 \\ b_3 \\ b_4 \end{bmatrix} \tag{49}$$

where b_i is the bias of gyro number i.

Augmented Gyro Error Model

The total gyro error is the sum of all of the errors discussed before, namely, misalignment, scale factor, and bias errors, that is,

$$\Delta \boldsymbol{G} = \Delta \boldsymbol{G}^m + \Delta \boldsymbol{G}^k + \boldsymbol{b} \tag{50a}$$

or using Eqs. (44) and (48c),

$$\Delta \boldsymbol{G} = \Omega^m E \boldsymbol{d} + \Omega^k \boldsymbol{k} + \boldsymbol{b} \tag{50b}$$

The last equation can be written in the following form:

$$\boldsymbol{G}_a - C\boldsymbol{\omega}_b = \begin{bmatrix} \Omega^m E & \Omega^k & I_4 \end{bmatrix} \begin{bmatrix} \boldsymbol{d} \\ \boldsymbol{k} \\ \boldsymbol{b} \end{bmatrix} \tag{50c}$$

where I_4 is a fourth-order identity matrix. As mentioned before, $\boldsymbol{G}_n$ is the nominal angular velocity measured by the four gyros. The left-hand side of the last equation as well as the matrix on the right-hand side is a function of the body angular rate $\boldsymbol{\omega}_b$. We denote them as follows:

$$\boldsymbol{y}(\boldsymbol{\omega}_b) = \boldsymbol{G}_a - C\boldsymbol{\omega}_b \tag{51a}$$

$$H(\boldsymbol{\omega}_b) = \begin{bmatrix} \Omega^m E & \Omega^k & I_4 \end{bmatrix} \tag{51b}$$

Also let

$$\boldsymbol{x} = \begin{bmatrix} \boldsymbol{d} \\ \boldsymbol{k} \\ \boldsymbol{b} \end{bmatrix} \tag{51c}$$

then Eq. (50c) can be written as

$$\boldsymbol{y}(\boldsymbol{\omega}_b) = H(\boldsymbol{\omega}_b)\boldsymbol{x} \tag{51d}$$

Calibration-Parameters Estimation for Known Rate

Our goal now is to estimate $\boldsymbol{x}$, and for that we need to know the angular rate, which the gyros are set to measure. We distinguish between two major cases. One case is that where $\boldsymbol{\omega}_b$, the reference SC angular velocity, is known, and the other case is that where the rate is not known and has to be evaluated simultaneously with the estimate of $\boldsymbol{x}$. In the first case we also distinguish between the deterministic and stochastic cases. All of these cases are discussed next.

Deterministic Case

When the SC rotates at a certain angular rate and a one-time measurement of the four gyro readings is taken at that time, which we denote by t_k, we obtain one matrix equation, as follows:

$$\boldsymbol{y}(\boldsymbol{\omega}_{b,k}) = H(\boldsymbol{\omega}_{b,k})\boldsymbol{x} \tag{52}$$

where $\boldsymbol{\omega}_{b,k}$ is the angular rate at time t_k. This yields 4 equations for the 16 unknowns of $\boldsymbol{x}$. If the rate does not change, then more measurements do not change the equations. A change in the angular rate of the SC is needed to generate more equations. Note that, even if we have 16 equations, it does not mean that they are all independent and that we can solve for $\boldsymbol{x}$. We have to design the profile of $\boldsymbol{\omega}_b$ and the times when measurements are taken in such a way that we will be able to find 16 independent equations. Let us denote the 16 independent equations by one matrix equation as follows:

$$\tilde{\boldsymbol{y}} = \tilde{H}\boldsymbol{x} \tag{53}$$

Because we have 16 independent equations, $\tilde{H}$ has an inverse; therefore, we can solve for $\boldsymbol{x}$ using

$$\boldsymbol{x} = \tilde{H}^{-1}\tilde{\boldsymbol{y}} \tag{54}$$

Stochastic Overdetermined Case

In this case, we assume that the measurements are contaminated by noise, which is the most likely case. Therefore, the matrix equation that describes this case at time t_k is

$$\boldsymbol{y}(\boldsymbol{\omega}_{b,k}) = H(\boldsymbol{\omega}_{b,k})\boldsymbol{x} + \boldsymbol{v}_k \tag{55}$$

Even if we find 16 independent equations from measurements done at different time points, we still want to use more measurements and obtain $\boldsymbol{x}$ as a least-squares estimate. For n measurement points, we have

$$\begin{bmatrix} \boldsymbol{y}(\boldsymbol{\omega}_{b,1}) \\ \boldsymbol{y}(\boldsymbol{\omega}_{b,2}) \\ \vdots \\ \boldsymbol{y}(\boldsymbol{\omega}_{b,n}) \end{bmatrix} = \begin{bmatrix} H(\boldsymbol{\omega}_{b,1}) \\ H(\boldsymbol{\omega}_{b,2}) \\ \vdots \\ H(\boldsymbol{\omega}_{b,n}) \end{bmatrix} \boldsymbol{x} + \begin{bmatrix} \boldsymbol{v}_1 \\ \boldsymbol{v}_2 \\ \vdots \\ \boldsymbol{v}_n \end{bmatrix} \tag{56}$$

Let

$$\boldsymbol{Y} = \begin{bmatrix} \boldsymbol{y}(\boldsymbol{\omega}_{b,1}) \\ \boldsymbol{y}(\boldsymbol{\omega}_{b,2}) \\ \vdots \\ \boldsymbol{y}(\boldsymbol{\omega}_{b,n}) \end{bmatrix} \tag{57a}$$

$$\boldsymbol{H} = \begin{bmatrix} H(\boldsymbol{\omega}_{b,1}) \\ H(\boldsymbol{\omega}_{b,2}) \\ \vdots \\ H(\boldsymbol{\omega}_{b,n}) \end{bmatrix} \tag{57b}$$

and let R be the covariance matrix of the noise vector $\boldsymbol{V} = [\boldsymbol{v}_1^T \cdots \boldsymbol{v}_n^T]^T$ then $\hat{\boldsymbol{x}}$, the weighted-least-squares estimate of $\boldsymbol{x}$, is as follows[8]:

$$\hat{\boldsymbol{x}} = (H^T R^{-1} H)^{-1} H^T R^{-1} \boldsymbol{Y} \tag{58}$$

The profile of $\boldsymbol{\omega}_b$ has to be chosen in a careful way as to enhance the observability of $\boldsymbol{x}$.

Calibration-Parameters Estimation for Unknown Rate

In this case, we have to find the angular rate vector while estimating the calibration parameters. The information that we have is attitude information and gyro measurements. We need the attitude information to estimate the angular rate, and we need the gyro measurements, as well as the estimated angular rate, for the calibration process. The attitude information can be supplied in various ways, namely, we may have it in the form of raw vector measurements or we may have it in an already processed form as attitude quaternion, for example. The angular rate behaves according to the following SC angular dynamics equation[9]:

$$\dot{\boldsymbol{\omega}} = I^{-1}[(I\boldsymbol{\omega} + \boldsymbol{h})\times]\boldsymbol{\omega} + I^{-1}(\boldsymbol{T} - \dot{\boldsymbol{h}}) \tag{59a}$$

where I is the SC inertia tensor, $[(I\boldsymbol{\omega} + \boldsymbol{h})\times]$ is the cross-product matrix of the vector $(I\boldsymbol{\omega} + \boldsymbol{h})$, $\boldsymbol{h}$ is the angular momentum of the momentum wheels, and $\boldsymbol{T}$ is the external torque operating on the SC. Because $\boldsymbol{x}$ is a constant vector, it obeys the following differential equation:

$$\dot{\boldsymbol{x}} = 0 \tag{59b}$$

We are tempted to combine the last two equations into one dynamics equation as follows:

$$\begin{bmatrix}\dot{\omega}\\ \dot{x}\end{bmatrix}=\begin{bmatrix}I^{-1}[(I\omega+h)\times] & 0\\ 0 & 0\end{bmatrix}\begin{bmatrix}\omega\\ x\end{bmatrix}+\begin{bmatrix}I^{-1}(T-\dot{h})\\ 0\end{bmatrix} \tag{59c}$$

This dynamics model calls for the use of a KF. In fact, the most appropriate filter is the pseudolinear Kalman (PSELIKA) filter.[10] To find the suitable measurement equation, we turn to Eqs. (50c) and (51b) from which it is obvious that

$$G_a=[C \quad H(\omega)]\begin{bmatrix}\omega\\ x\end{bmatrix} \tag{60}$$

To apply the filter algorithm, we need to add some process noise to Eq. (59c) and some measurement noise to Eq. (60). The use of the dynamics model of Eq. (59c) and the gyro measurements G_a alone in a KF is not sufficient for estimating x. The reason is that to estimate x we need accurate knowledge of the true angular velocity in addition to the angular velocity measurement supplied by the gyros. Although the latter is available, the former cannot be obtained accurately enough from the SC dynamics unless attitude measurements are available. As mentioned, attitude can be given in several ways, namely, it can be given in a raw form as vector measurements or in processed attitude parameters like a quaternion or direction cosine matrix (DCM). Let us consider two typical cases, one where attitude is represented by a processed quaternion and the other case when we have raw vector measurements. The case where attitude is given in the form of a DCM can be inferred from the development presented in Ref. 11 and the way we handle quaternion representation of attitude.

Estimation When Attitude Is Presented by the Attitude Quaternion

Let us assume first that the attitude is given in a form of a quaternion.[12] In this case, the filter dynamics is as follows[11]:

$$\begin{bmatrix}\dot{\omega}\\ \dot{x}\\ \dot{q}\end{bmatrix}=\begin{bmatrix}I^{-1}[(I\omega+h)\times] & 0 & 0\\ 0 & 0 & 0\\ \frac{1}{2}Q & 0 & 0\end{bmatrix}\begin{bmatrix}\omega\\ x\\ q\end{bmatrix}+\begin{bmatrix}I^{-1}(T-\dot{h})\\ 0\\ 0\end{bmatrix} \tag{61}$$

where

$$Q=\begin{bmatrix}q_4 & -q_3 & q_2\\ q_3 & q_4 & -q_1\\ -q_2 & q_1 & q_4\\ -q_1 & -q_2 & -q_3\end{bmatrix} \tag{62}$$

and the corresponding measurement equation is

$$q_m=[0_{4\times 3} \quad 0_{4\times 16} \quad I_{4\times 4}]\begin{bmatrix}\omega\\ x\\ q\end{bmatrix} \tag{63}$$

Like I_4, the matrix $I_{4\times 4}$ is a fourth-order identity matrix. The combined measurement equation consists of Eqs. (60) and (63), that is,

$$\begin{bmatrix}G_a\\ q_m\end{bmatrix}=\begin{bmatrix}C & H(\omega) & 0_{4\times 4}\\ 0_{4\times 3} & 0_{4\times 16} & I_{4\times 4}\end{bmatrix}\begin{bmatrix}\omega\\ x\\ q\end{bmatrix} \tag{64}$$

Estimation When Attitude Is Given by Vector Observations

Traditionally, in space missions, attitude was determined from vector observations. These observations can be used directly to check the divergence of the angular velocity estimates.[11] This is shown next. Suppose that we have N vector measurements at a certain time point. Let r_i be some abstract ith vector as expressed in the reference coordinate system, and let b_i be the same vector when expressed in the body coordinates. From the laws of kinematics it is known that

$$A\dot{r}_i=\dot{b}_i+\omega\times b_i \tag{65}$$

where $\dot{r}_i$ is the time derivative of r_i as seen by an observer in the reference coordinates, A is the matrix that transforms vectors from the reference to body coordinates, and $\dot{b}_i$ is the time derivative of b_i as seen by an observer in body coordinates. The vector b_i is a measured vector, and $\dot{b}_i$ is its time derivative. We can write Eq. (65) as follows:

$$\dot{b}_i=[b_i\times]\omega+A\dot{r}_i \tag{66}$$

Note that $\dot{r}_i$ is computable inasmuch as r_i is usually known because, generally, the vector is a direction to a certain known planet whose location is given in an Almanac or, as with magnetometer measurements, the vector can be computed using a model. (Note that quite often the rate of change of r_i is so small that $\dot{r}_i$ is negligible). Define

$$\dot{\beta}=\begin{bmatrix}\dot{b}_1\\ \cdot\\ \cdot\\ \dot{b}_N\end{bmatrix} \tag{67a}$$

$$B=\begin{bmatrix}[b_1\times]\\ \cdot\\ \cdot\\ [b_N\times]\end{bmatrix} \tag{67b}$$

$$u=\begin{bmatrix}A\dot{r}_1\\ \cdot\\ \cdot\\ A\dot{r}_N\end{bmatrix} \tag{67c}$$

then we can augment all of the N equations of Eq. (66) into one matrix equation as follows:

$$\dot{\beta}=B\omega+u \tag{68}$$

Therefore, instead of Eq. (61), we obtain in this case of vector measurement the augmented equation

$$\begin{bmatrix}\dot{\omega}\\ \dot{x}\\ \dot{\beta}\end{bmatrix}=\begin{bmatrix}I^{-1}[(I\omega+h)\times] & 0 & 0\\ 0 & 0 & 0\\ B & 0 & 0\end{bmatrix}\begin{bmatrix}\omega\\ x\\ \beta\end{bmatrix}+\begin{bmatrix}I^{-1}(T-\dot{h})\\ 0\\ u\end{bmatrix} \tag{69}$$

and the corresponding measurement equation is

$$\beta_m=[0_{3N\times 3} \quad 0_{3N\times 16} \quad I_{3N\times 3N}]\begin{bmatrix}\omega\\ x\\ \beta\end{bmatrix} \tag{70}$$

whereas the augmented measurement equation is

$$\begin{bmatrix}G_a\\ \beta_m\end{bmatrix}=\begin{bmatrix}C & H(\omega) & 0_{3N\times 3N}\\ 0_{3N\times 3} & 0_{3N\times 16} & I_{3N\times 3N}\end{bmatrix}\begin{bmatrix}\omega\\ x\\ \beta\end{bmatrix} \tag{71}$$

Although it was not mentioned earlier, note that, to apply a KF using the aforementioned models, white noise has to be added to the dynamics and measurement models. The noise accounts for an imperfect dynamics model and for measurement noise.

Compensation

To complete the calibration process we need to perform its second stage, namely, compensation, where we eliminate the estimated errors from the gyro readings. From Eq. (50c), we obtain

$$C\omega_b=G_a-\begin{bmatrix}\Omega^m E & \Omega^k & I_4\end{bmatrix}\begin{bmatrix}d\\ k\\ b\end{bmatrix} \tag{72a}$$

As mentioned before, G_a is a vector of the gyro readings and ω_b is the (correct) angular velocity vector expressed in body axes. However,

we do not have ω_b, which is what we are trying to measure; therefore, to compute Ω^m and Ω^k, which have to be computed using ω_b, we use the measured uncompensated angular rate vector, which is derived from the uncompensated gyro measurements that we called actual and denoted by a. Alternatively, we can use $\hat{\omega}$, the estimated angular rate vector. Also, we do not have the actual values of $\boldsymbol{d}$, $\boldsymbol{k}$, or $\boldsymbol{b}$, but rather their estimate; therefore, using the values on hand, Eq. (72a) becomes

$$C\hat{\omega}_b = \boldsymbol{G}_a - \begin{bmatrix}\Omega_a^m E & \Omega_a^k & I_4\end{bmatrix}\begin{bmatrix}\hat{\boldsymbol{d}}\\ \hat{\boldsymbol{k}}\\ \hat{\boldsymbol{b}}\end{bmatrix} \tag{72b}$$

where a denotes the actual values and the caret denotes estimated vectors. Alternatively, we can use $\hat{\omega}$ and obtain

$$C\hat{\omega}_b = \boldsymbol{G}_a - \begin{bmatrix}\hat{\Omega}^m E & \hat{\Omega}^k & I_4\end{bmatrix}\begin{bmatrix}\hat{\boldsymbol{d}}\\ \hat{\boldsymbol{k}}\\ \hat{\boldsymbol{b}}\end{bmatrix} \tag{72c}$$

To obtain the compensated measurements of the angular rate vector define the M matrix as follows:

$$M = \begin{bmatrix}1 & 0 & 0\\ 0 & 1 & 0\\ 0 & 0 & \frac{1}{2}\end{bmatrix} \tag{73}$$

It is easy to verify that

$$MC^TC = I \tag{74}$$

Therefore, premultiplying Eq. (72b) by MC^T yields

$$\hat{\omega}_b = MC^T\boldsymbol{G}_a - MC^T\begin{bmatrix}\Omega_a^m E & \Omega_a^k & I_4\end{bmatrix}\begin{bmatrix}\hat{\boldsymbol{d}}\\ \hat{\boldsymbol{k}}\\ \hat{\boldsymbol{b}}\end{bmatrix} \tag{75a}$$

or when using Eq. (72c)

$$\hat{\omega}_b = MC^T\boldsymbol{G}_a - MC^T\begin{bmatrix}\hat{\Omega}^m E & \hat{\Omega}_k & I_4\end{bmatrix}\begin{bmatrix}\hat{\boldsymbol{d}}\\ \hat{\boldsymbol{k}}\\ \hat{\boldsymbol{b}}\end{bmatrix} \tag{75b}$$

Simulation Results

To examine the new calibration process, a simulator was developed to produce the gyro, reaction wheel, and star tracker data. Much care was devoted to the simulation because any dynamics errors would be perceived by the KF as a state estimation error. A maneuver strategy was developed to enhance the observability of the calibration parameters. The angular rate profile that resulted is shown in Fig. 5. This particular sequence of rotations was chosen to enhance the observability of the calibration parameters. Accordingly, the sequence is started with a zero maneuver during which the bias is estimated and removed if so desired. Next, the SC is rotated about a gyro input axis. During this time period, the scale factor of that gyro can be estimated, as well as the misalignment of the orthogonal gyros, and so on. White noise was added to the readings of the four gyros and to the measured quaternion. The gyro noise

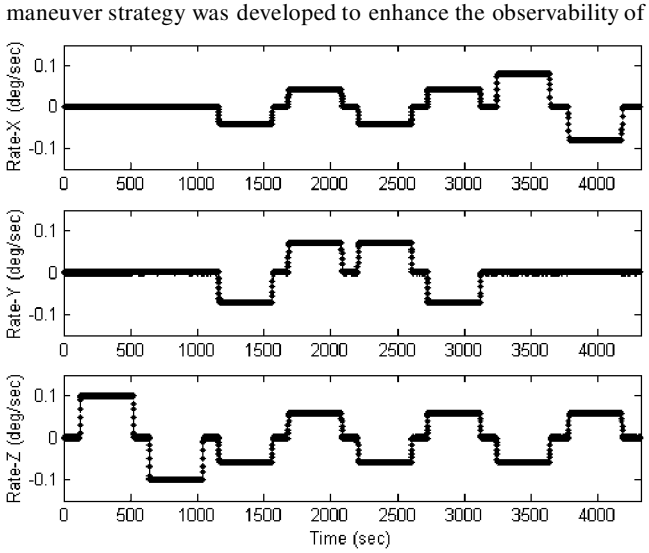

Fig. 5 SC calibration angular rate maneuvers.

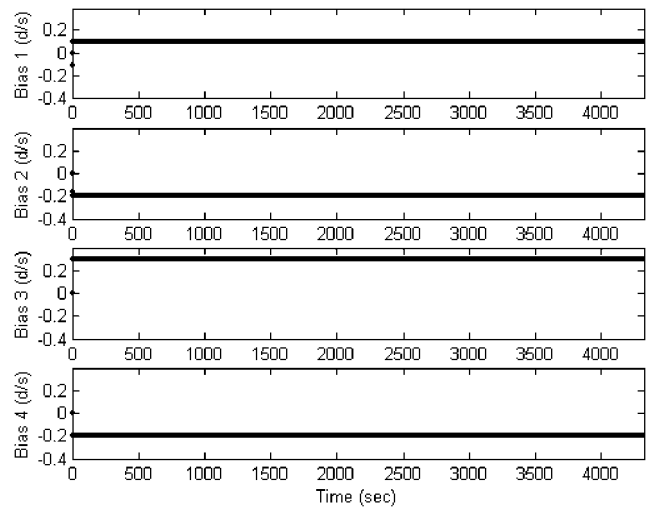

Fig. 6 Gyro bias estimate (bold) vs truth (covered by the former).

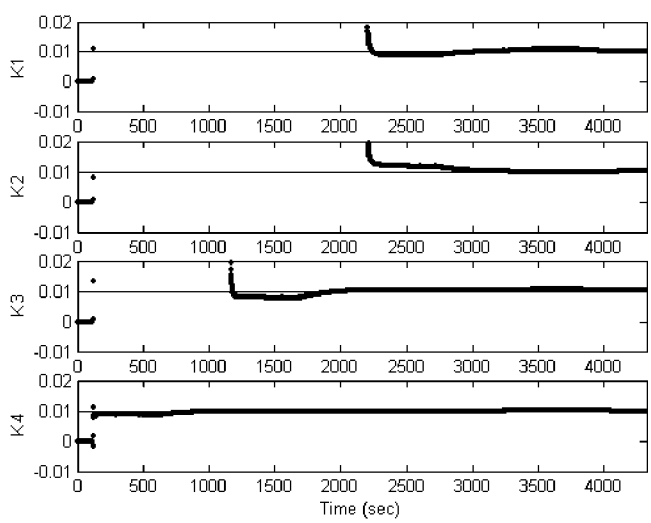

Fig. 7 Gyro scale factor estimate (bold) vs truth (thin).

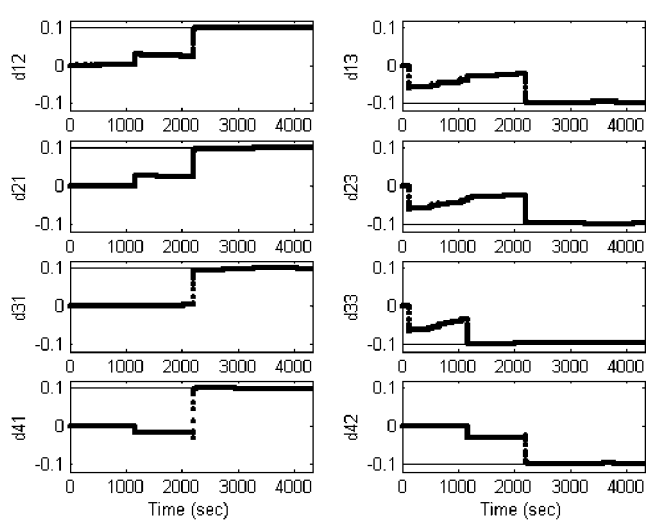

Fig. 8 Gyro misalignment estimate (bold) vs truth (thin).

was drawn from a random number generator that generated uniformly distributed random numbers between −0.8 and 0.8 deg/h. The quaternion measurement error was also simulated as a uniformly distributed noise between -10^{-5} and 10^{-5} for each of the four quaternion components. Measurement update was performed every second.

The KF was then executed on the simulated data. The biases were estimated using the initial inertial period. The scale factor and misalignments influenced by a rotation about a given axis were observable and estimated when a maneuver was performed about that axis. All states were estimated with less than a 1% deviation from truth. The KF bias estimate can be seen in Fig. 6. The scale factor estimate is presented in Fig. 7, and the misalignment estimate in Fig. 8.

Conclusions

We presented a new method of gyro calibration. Normally, we have to calibrate a cluster of three gyros whose sensitive axes are along the body axes. Here, the rate is read by four gyros only one of which is aligned along the body coordinate axes. Therefore, a new algorithm was devised for calibrating a skewed quadruplet rather than the customary triad gyro set whose axes are aligned along the body coordinate axes. In particular, a new model had to be developed for the gyro misalignment errors. Normally, the gyro outputs are used to supply data for a differential equation, which is solved to compute attitude. With the new method, the gyro outputs are used as measurements, which are fed into a PSELIKA filter. The filter uses attitude measurements, in the form of quaternions, and the SC dynamics equation to estimate the gyro misalignment, scale factors, and biases. The new calibration algorithm was developed in particular for the calibration of the EOS-AQUA satellite gyros. The effectiveness of the new algorithm was demonstrated through simulations with error of each estimated parameter being less than 1%.

Appendix: Example of Classical Gyro Arrangement

We consider a particular customary gyro arrangement, where the sensitive axes of all four gyros coincide with one of the body axes. The purpose of this example is to show that the general case treated in the paper reduces in this case to well-known results.

Consider the four-gyro arrangement presented in Fig. A1. The gyros G_1, G_2, and G_4, are aligned along the body x, y, and z axes, respectively, and the G_3 gyro is aligned along the negative body y axis. Using Eqs. (38) with $\gamma = 0$ deg, we obtain the E matrix and $\boldsymbol{d}$ for gyro 1 as

$$E_1 = \begin{bmatrix} 0 & 0 \\ 1 & 0 \\ 0 & 1 \end{bmatrix} \tag{A1a}$$

$$\boldsymbol{d}_1 = \begin{bmatrix} d_{1y} \\ d_{1z} \end{bmatrix} \tag{A1b}$$

Using Eqs. (23) with $\alpha = 0$ deg and $\beta = 0$ deg, we obtain the E matrix and $\boldsymbol{d}$ for gyro 2 as

$$E_2 = \begin{bmatrix} 1 & 0 \\ 0 & 0 \\ 0 & 1 \end{bmatrix} \tag{A2a}$$

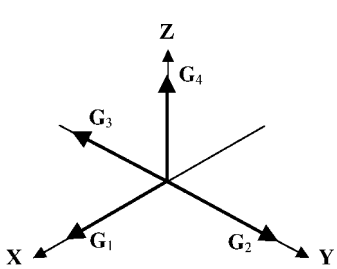

Fig. A1 Special gyro arrangement.

$$\boldsymbol{d}_2 = \begin{bmatrix} d_{2x} \\ d_{2z} \end{bmatrix} \tag{A2b}$$

In a similar way, using $\alpha = 0$ deg and $\beta = 0$ deg in Eqs. (31), we obtain the corresponding E and $\boldsymbol{d}$ for the third gyro, which is aligned along the negative y axis:

$$E_3 = \begin{bmatrix} -1 & 0 \\ 0 & 0 \\ 0 & 1 \end{bmatrix} \tag{A3a}$$

$$\boldsymbol{d}_3 = \begin{bmatrix} d_{3x} \\ d_{3z} \end{bmatrix} \tag{A3b}$$

Finally, the orientation of G_4 of this special case is identical to that of the AQUA G_4 gyro. Therefore, from Eqs. (42),

$$E_4 = \begin{bmatrix} 1 & 0 \\ 0 & 1 \\ 0 & 0 \end{bmatrix} \tag{A4a}$$

$$\boldsymbol{d}_4 = \begin{bmatrix} d_{4x} \\ d_{4y} \end{bmatrix} \tag{A4b}$$

Using these four E_i matrices and the four $\boldsymbol{d}_i$ column matrices in Eqs. (43), we obtain from Eq. (44)

$$\Delta \boldsymbol{G}^m = \Omega^m E \boldsymbol{d}$$

$$= \begin{bmatrix} \omega_y & \omega_z & 0 & 0 & 0 & 0 & 0 & 0 \\ 0 & 0 & \omega_x & \omega_z & 0 & 0 & 0 & 0 \\ 0 & 0 & 0 & 0 & -\omega_x & \omega_z & 0 & 0 \\ 0 & 0 & 0 & 0 & 0 & 0 & \omega_x & \omega_y \end{bmatrix} \begin{bmatrix} d_{1y} \\ d_{1z} \\ d_{2x} \\ d_{2z} \\ d_{3x} \\ d_{3z} \\ d_{4x} \\ d_{4y} \end{bmatrix} \tag{A5}$$

This is the correct misalignment error that can be easily reasoned for the gyro arrangement of Fig. A1.

References

[1]Chatfield, A. B., *Fundamentals of High Accuracy Inertial Navigation*, Vol. 174, Progress in Astronautics and Aeronautics, AIAA, Reston, VA, 1997, pp. 93–106.

[2]Bar-Itzhack, I. Y., and Harman, R. R., "True Covariance Simulation of the EUVE Update Filter," *Proceedings of the 1989 Flight Mechanics Estimation Theory Symposium*. NASA CP 3050, 1989, pp. 223–236.

[3]Deutschmann, J. K., and Bar-Itzhack, I. Y., "Evaluation of Attitude and Orbit Estimation Using Actual Earth Magnetic Field Data," *Journal of Guidance, Control, and Dynamics*, Vol. 24, No. 3, 2001, pp. 616–623.

[4]Gray, C. W., Herman, L. K., Kolve, D. I., and Westerlund, G. L., "On-Orbit Attitude Reference Alignment and Calibration," *Advances in the Astronautical Sciences*, Vol. 72, 1990, pp. 275–289; also American Astronautical Society, AAS Paper 90-042, 1990.

[5]Hashmall, J. A., Radomski, A., and Sedlak, J., "On-Orbit Calibration of Satellite Gyroscopes," AIAA Paper 2000-4244, Aug. 2000.

[6]Shuster, M. D., "Inflight Estimation of Spacecraft Sensor Alignment," American Astronautical Society, AAS Paper 90-041, Feb. 1990.

[7]Lambertson, M., Keat, J., and Scheidker, E., "Multimission Three-Axis Stabilized Spacecraft (MTASS) Flight Dynamics Support System (FDSS) Mathematical Background," NASA Goddard Space Flight Center, Publ. 553-FDD-93/032R0UD0, Sept. 1993, pp. 3.3.2-1–3.3.2-10.

[8]Gelb, A., (ed.), *Applied Optimal Estimation*, MIT Press, Cambridge, MA, 1974, p. 103.

[9]Wertz, J. R. (ed.), *Spacecraft Attitude Determination and Control*, D. Reidel, Dordrecht, The Netherlands, 1984, p. 523.

[10]Harman, R. R., and Bar-Itzhack, I. Y., "Pseudolinear and State-Dependent Riccati Equation Filters for Angular Rate Estimation," *Journal of Guidance, Control, and Dynamics*, Vol. 22, No. 5, 1999, pp. 723–725.

[11]Bar-Itzhack, I. Y., "Classification of Algorithms for Angular Velocity Estimation," *Journal of Guidance, Control, and Dynamics*, Vol. 24, No. 2, 2001, pp. 214–218.

[12]Azor, R., Bar-Itzhack, I. Y., Deutschmann, J. R., and Harman, R. R., "Angular-Rate Estimation Using Delayed Quaternion Measurements," *Journal of Guidance, Control, and Dynamics*, Vol. 24, No. 3, 2001, pp. 436–443.